Surface Science 707 (2021) 121797

Contents lists available at ScienceDirect

Surface Science

journal homepage: www.elsevier.com/locate/susc

The sputtering of radiolytic O_2 in ion irradiated H_2O-ice

Patrick D. Tribbett [*,a], Mark J. Loeffler [a,b]

[a] Department of Astronomy and Planetary Science, Northern Arizona University, Box 6010, Flagstaff, AZ 86011, USA
[b] Center for Materials Interfaces in Research and Applications (MIRA), Northern Arizona University, Box 6010, Flagstaff, AZ 86011, USA

ARTICLE INFO

Keywords:
Sputtering
Water ice
Low energy ions
Radiolysis
Europa

ABSTRACT

Charged particle bombardment alters the physical and chemical properties of extraterrestrial icy surfaces by simultaneously producing radiolytic products and sputtered material. To better understand these phenomena, we measure the total sputtering yield of H_2O-ice induced by 0.5–5 keV Ar^+ at temperatures between 40 and 120 K, using microbalance gravimetry as our analytical tool. In addition, we also estimate the sputtered flux of radiolytic products formed during irradiation and in both cases find good agreement with comparable laboratory studies. At 120 K, we find that the O_2/H_2O sputtered ratio increases nearly linearly with the ion range suggesting that the ions are stopping at depths where O_2 is still efficiently being produced below the surface. Furthermore, we find that although theoretical models appear to over predict our O_2 sputtering yields by about a factor of three, we can make a small adjustment to this model, which improves the agreement between the model and the laboratory data significantly. This empirical adjustment may have implications for models of energetic processing that occurs on extraterrestrial icy surfaces, such as Europa, where low-energy ions are thought to be the primary source producing O_2 from sputtering of the surface H_2O-ice.

1. Introduction

Planetary surfaces with absent or tenuous atmospheres are irradiated with charged particles. These particles can significantly alter the composition of the surface, as well as erode the surface through processes including sputtering. Sputtering occurs when incoming particles collisionally remove material (nuclear or elastic sputtering), electronically excite and eject material (electronic sputtering), or produce and consequently release radiolytic products [1–3]. Sputtering by magnetospheric charged particles is responsible for the production of extended atmospheres around the Jovian and Saturnian icy satellites [4–6]. For this reason, the sputtering of H_2O-ice via energetic ions has been extensively studied, particularly for hydrogen, helium, and argon ions [2,7–15]. Additionally, electrons have been shown to erode surfaces through sputtering [16–19]. However, few have quantified the sputtering yields of lower energy heavy ions [7,8,10,14,15,20], which are a substantial population of the charged particles within the Jovian magnetospheric plasma [21].

Sputtering is quantified by a term known as the sputtering yield (Y) or the number of ejected molecules, atoms, or ions per incident particle. Nuclear sputtering occurs through billiard ball style collisions resulting in the removal of material [1]. Electronic sputtering occurs through repulsive interactions between atoms when collisional energy is transferred to electronic energy promoting electrons to anti-bonding orbitals [22]. Y is dependent on the projectiles's nuclear (S_N) and electronic stopping cross section (S_e); $S = \frac{1}{N}\frac{dE}{dx}$, where dE/dx is the differential loss in energy per unit path length, and N is the number density of the target. Early studies found that Y varied approximately linearly with S_N for solids, and when S_N is dominant the sputtering yield followed predictions by linear cascade theory [1]. However for insulating ices like H_2O, it was later shown that $Y \propto S_e^2$, and consideration of exclusively nuclear stopping cross sections results in drastic underestimations of Y [23]. Moreover, in H_2O electronic sputtering dominates at larger ion energies (>10 keV) [9]. Lower ion energies (<10 keV) are dominated by nuclear sputtering, or some combination of nuclear and electronic sputtering. Few studies have focused on this transitional region between nuclear and electronic dominated sputtering [7,10,14,20].

Sputtering yields of H_2O-ice induced by low energy (0.5–6 keV) H^+ and Ne^+ at a wide range of temperatures (30–140 K) were first quantified employing a calibrated quadrupole mass filter by Bar-Nun et al. [14]. Their study confirmed a nuclear sputtering mechanism for Ne^+ and demonstrated a transition from a nuclear to electronic mechanism for H^+ within the energy range studied. Additionally, temperature dependent fluxes of ejected O_2 and H_2 were identified. Furthermore, Y was

* Corresponding author.
E-mail address: pdt43@nau.edu (P.D. Tribbett).

https://doi.org/10.1016/j.susc.2021.121797
Received 5 June 2020; Received in revised form 29 December 2020; Accepted 31 December 2020
Available online 4 January 2021

observed to be constant at temperatures less than 80 K but increased above 80 K, which is consistent with trends seen for higher (MeV) energy ions and believed to be a result of the increased production of radiolytic O_2 and H_2 [24,25]. Soon after, Christensen et al. 1986 quantified sputtering yields for 2–6 keV Ar^+, Ne^+, N^+, He^+, and e^-, at 78 K. These yields were calculated based on resulting impact crater diameter [7]. They found that sputtering yields of H_2O-ice at these lower energies agree fairly well with Sigmund's linear cascade theory for collisional sputtering. Famá et al. 2008 confirmed a sputtering yield enhancement at temperatures greater than 80 K for low energy Ar^+, which they also attributed to the increased production of O_2 [10]. Additionally, Famá et al. developed a theoretical model to predict sputtering yields of H_2O-ice. This semi-analytical model has been validated using a compilation of data from references [7,10,15,23,26]. More recently, Teolis et al. 2017 generalized Famá's model for total sputtering yield, to predict sputtering yields of different ejected species including H_2, O_2, and H_2O [27].

Interestingly, laboratory studies have also shown that the concentration of radiolytic O_2 is not constant with depth below the surface ice but reaches a maximum somewhere within the first 100 ML (~300 Å) below the surface [11,28]. Examining this surface region in more detail using low energy ions will give direct insight into the concentration profile of radiolytic O_2. In addition, it will also test how well theoretical models predict values for O_2 sputtered from H_2O-ice in this energy range, which is of particular interest to the astronomical community, as ions in this energy range are thought to be the main producer of exospheres around icy satellites [20,21]. Thus, here we investigate the sputtering yield of H_2O-ice induced by 0.5–5 keV Ar^+ at temperatures between 40 K and 120 K, using microbalance gravimetry as our analytical technique. We compare our H_2O sputtering yields to previous work, as well as to predictions made by the Famá et al. 2008 sputtering model. Additionally, we estimate the sputtered flux of radiolytically produced O_2 and compare those estimates to the values predicted by the Teolis et al. 2017 model, giving possible explanations for any observed deviations between the laboratory data and theoretical predictions.

2. Experimental methods

2.1. Experimental setup

All sputtering yield measurements were performed in a stainless steel ultra-high vacuum chamber with a base pressure of 2.5×10^{-9} Torr (Fig. 1); we estimate that the pressure at the sample is significantly lower given that it is protected by a thermal-radiation shield. To prepare our samples, we vapor deposited H_2O-ice at 100 K at normal incidence onto an optically flat gold mirror electrode of an Inficon IC6 quartz-crystal microbalance (QCM) as in our previous studies [29]. Under these conditions, the sample is amorphous and lacks significant microporosity [30,31]. Ice films were grown at a rate of 2×10^{15} H_2O cm^{-2} s^{-1} to a column density of $2.9 \pm 0.1 \times 10^{18}$ molecules cm^{-2} (~ 0.87 μm), unless otherwise stated. Film thicknesses given in this paper were estimated from our QCM-derived column densities, assuming a density of 1 g cm^{-3} for H_2O-ice. We chose this value for the density, so that parameters derived from our modeling efforts (see Section 3.4) would be directly comparable to previous work [27]. The QCM stability enabled us to be sensitive to changes of 0.1 Hz (~ 5×10^{13} molecules cm^{-2}).

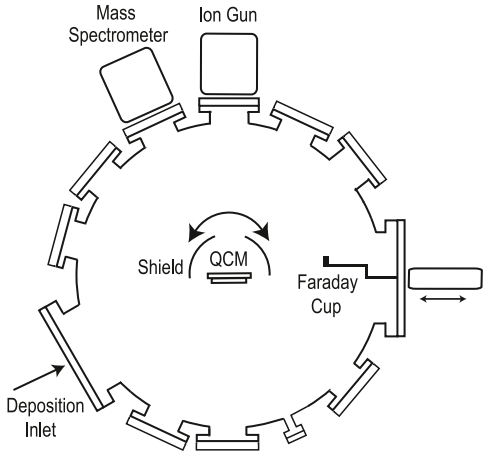

Fig. 1. Experimental setup along the sample holder axis.

After growth, the H_2O-ice was cooled to the desired temperature and irradiated with Ar^+ (0.5–5 keV) at normal incidence using a differentially-pumped Non Sequitur electron impact ionization gun (Model 1401). To ensure uniform irradiation of the sample, the ion beam was externally rastered with a BK Precision 4050 Series Function/Arbitrary Waveform Generator. Optimal peak to peak function voltages and the raster frequency were determined based on the uniformity of the full width half maximum (FWHM) of the ion beam for each ion energy used in this study. Typical fluxes, measured by a Faraday Cup, were ~ 1×10^{13} ions cm^{-2} s^{-1}. Secondary electrons produced by ion impacts within the Faraday cup were prevented from leaving the cup by biasing it in series with the electrometer with +9 V. During the experiment, the ion flux was monitored with a thin wire placed in the beam path and biased at -9 V. The current typically varied by less than 10% during the experiment.

2.2. Calculating the total sputtering yield

Sputtering yields were calculated based on the changes in output frequency of the QCM during irradiation (df/dt), as described in Meier and Loeffler 2020 [16]. The change in areal mass is related the change in QCM frequency by:

$$\frac{dQ}{dt} = \frac{-k\frac{df}{dt}}{f^2} \tag{1}$$

where Q is the areal mass of the ice film, f is the frequency at which the derivative is evaluated, and k is a constant (4.417×10^5 Hz g cm^{-2}) [32]. Assuming the impactor flux (Φ) is constant and the total mass loss is due to H_2O, Y_{H_2O} can be calculated by:

$$Y_{H_2O} = \frac{\frac{dQ}{dt}}{\Phi}\left(\frac{N_A}{M_{H_2O}}\right) \tag{2}$$

where N_A is Avogadro's number, and M_{H_2O} is the molar mass of water (18 g/mol). The measured value of df/dt was determined after a fluence of ~ 2×10^{15} ions cm^{-2} to ensure that sputtered flux from our sample had reached equilibrium. As was most easily seen in our higher temperature experiments (data not shown here), this chosen fluence is well past the point where df/dt has stopped increasing with fluence. This increase at low fluences has previously been attributed to the production of radiolytic H_2 and O_2 [11]. We note that while we present the total yield in terms of H_2O both for simplicity and for ease of comparison with previous experiments [10], we also consider the contribution from the main radiolytically produced species (Section 2.3 for more details).

2.3. Calculating the total O_2 sputtering yield

The sputtered flux of stable radiolytic species from from H_2O-ice mainly consists of H_2O, O_2, and H_2 [14,24,25,28,33]. Below 80 K, the flux consists primarily of H_2O and the sputtering yield is relatively constant [34]. Between 80 K and 130 K, the yield increases as a result of the radiolytic production of O_2 and H_2. Thus, as we are determining the sputtering yield via mass loss on our QCM, the changes we observe are predominantly due to the ejection of H_2O, O_2, and H_2. To provide estimates for the absolute O_2 sputtering yield, we used a two-tiered

approach. First, to estimate the amount of O_2 in the sputtered flux where the total yield has been shown to be independent of temperature ($\leq$ 80 K), we use the model prediction given in [27] (see Fig. 6 in [27]) for S^+ ions, which are expected to sputter in a similar manner to Ar^+ ions [27]. We used this model to estimate the O_2 component, after taking into account contribution from H_2. We utilized this approach rather than a fixed ratio for all energies, because differences in previous laboratory studies suggest that the O_2/H_2O ratio in the sputtered flux depends on energy and ion type [11,14,34]. The model-derived O_2/H_2O ratio at each energy studied here is given in Table 1. At irradiation temperatures higher than 80 K, we assume that any increase in the mass loss at a given energy compared with the average mass loss of our 40 and 80 K experiments (which were within ~ 5 % of one another) is exclusively due to O_2 and H_2, and that these products are produced and sputtered stoichiometrically [11,14,34]. This "enhanced" O_2 is then added to the average O_2 sputtered at 40 and 80 K ("intrinsic" O_2) to produce the total O_2 sputtering yield. For reference, we also give the O_2/H_2O ratios derived at 100 and 120 K for each energy in Table 1. Based on stoichiometry, the values for the H_2/H_2O are assumed to be twice that of those given for O_2 in Table 1.

2.4. Theoretical models

Experimental results of this study and several references herein are compiled and compared to the total sputtering yield model derived in [10]. Specifically, theoretical sputtering yields are computed using:

$$Y_{H_2O}(E, m_1, Z_1, \theta, T) = \frac{1}{U_0}\left(\frac{3}{4\pi^2 C_0}\alpha S_N + \eta S_e^2\right) \times \left(1 + \frac{Y_1}{Y_0} e^{-E_a/k_b T}\right) cos^{-f}(\theta) \quad (3)$$

where Z_1 is the atomic number of the projectile, m_1 is the mass of the projectile, U_0 is the surface binding energy of water, C_0 describes elastic scattering in a binary collision approximation, k_b is Boltzmann's constant, f is the empirically derived angular dependence, and E_a is a fitted temperature dependence constant. A detailed description of α and η can be found in [10].

We also compared our estimated experimental O_2 yields to predictions given by Teolis et al. 2017, who developed a general relation that predicts O_2 yields from the sputtering of H_2O-ice for a given energy (E), temperature (T) and incident angle (β). The derived expression is:

$$Y_{O_2}(E, T, \beta) = \epsilon g^0_{O_2} x_0 \left(1 - \exp\left(-\frac{r_0 \cos\beta}{x_0}\right)\right)\left(1 + q_0 \exp\left(-\frac{Q}{k_b T}\right)\right)(r_0 \cos\beta)^{-1} \quad (4)$$

where ϵ is the effective particle energy, which excludes energy contributing to lattice vibrations, $g^0_{O_2}$ is the surface radiolysis yield of O_2, x_0 is the approximate thickness of a surface layer that efficiently produces O_2, r_0 is the projectile range at a given incidence angle, q_0 describes the exponential temperature dependence, Q is the related to the effective activation energy, and k_b is Boltzmann's constant [27].

Table 1
O_2/H_2O ratios; [a] From Fig. 6 in [27]. [b] This work. [c] We note that this ratio is anomalously lower than the ratio at 40 and 80 K due to a larger uncertainty in the total mass loss.

Ion Energy (keV)	O_2/H_2O 40 and 80 K[a]	O_2/H_2O 100 K[b]	O_2/H_2O 120 K[c]
0.5	0.082	0.070[c]	0.143
0.75	0.107	0.114	0.169
1.0	0.121	0.204	0.200
2.0	0.164	0.239	0.331
3.0	0.184	0.241	0.384
4.0	0.215	0.233	0.414
5.0	0.223	0.311	0.512

We initially adopt values within the uncertainties of those used in [27] for $g^0_{O_2} = 0.005$ O_2 eV^{-1} $x_0 = 29$ Å, $q_0 = 10^3$ and Q = 0.06 eV. As $\epsilon = H \times E$, where H is the fraction of projectile energy available for radiolysis, we estimated ϵ by calculating H using SRIM [35]. We found that H ranged between 0.83 and 0.98 for projectile energies between 0.5 keV and 5 keV.

3. Results

3.1. Flux and thickness dependence of the total mass loss

A key goal of our study is to determine the effect of sputtering due to low energy ion bombardment at temperatures and energies relevant to extraterrestrial icy surfaces. Thus, we first needed to verify that our results were independent of the ion flux and sample thickness.

To investigate whether we were in a range where the Ar^+ flux effected the sputtering yield of H_2O-ice, we irradiated a 2.9×10^{18} H_2O cm^{-2} sample with 3 keV Ar^+ at 80 K with ion fluxes between 0.085 and 2×10^{13} ions cm^{-2} s^{-1}. As can be seen in Fig. 2, Y_{H_2O} is essentially constant over this range of fluxes.

There is also the potential that the sample thickness could effect the sputtering yield. For instance, it has been shown that Y_{H_2O} induced by energetic electrons increases when the penetration depth of the projectile is much greater than the film thickness [16]. We note that this effect will likely not be important in our studies, as the penetration depth of the Ar^+ is always significantly less than the film thickness (Table 2). However, previous studies have also demonstrated that ions can induce electrostatic charging of ice [36], which could potentially alter the sputtering yield. Thus, we irradiated samples of thicknesses between 60 nm and 1.2 μm with 3 keV Ar^+ at 80 K and measured Y_{H_2O}. As is shown in Fig. 3, there are no measurable variations in Y_{H_2O} over the range of thicknesses studied, suggesting that electrostatic charging effects are not significant enough in our experiments to alter the total sputtering yield, in agreement with previous work [10].

3.2. Energy and temperature dependence of the total mass loss

After determining that the total mass loss is independent of our chosen sample thickness and incident ion flux, we measured Y_{H_2O} for fresh samples of H_2O-ice (2.9×10^{18} H_2O cm^{-2}) as a function of Ar^+ energy at temperatures between 40 and 120 K (Fig. 4). We find that generally the total sputtering yield increases with temperature and energy, although this dependence in temperature is much more evident at the higher irradiation energies. For instance, at 5 keV, Y_{H_2O} is 1.14 times higher at 100 K and 1.41 times higher at 120 K than it is at 40 K.

To verify that our experimental sputtering yields were not systematically offset from an absolute sputtering yield, we compared our values

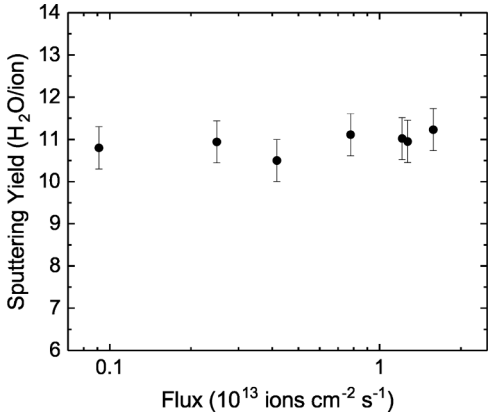

Fig. 2. Total sputtering yield for 2.9×10^{18} H_2O cm^{-2} samples irradiated with 3 keV Ar^+ at 80 K as a function of ion flux.

Table 2
Nuclear and electronic stopping powers, and projected ranges for argon ions used in this study calculated using SRIM assuming a density of 1 g cm^{-3} for H_2O [35].

Ion Energy (keV)	Nuclear Stopping Power eV/Å	Electronic Stopping Power eV/Å	Projected Range Å
0.5	17.86	1.30	40
0.75	20.89	1.59	50
1.0	23.15	1.83	58
2.0	28.79	2.59	87
3.0	32.02	3.17	112
4.0	34.17	3.66	135
5.0	35.71	4.10	156

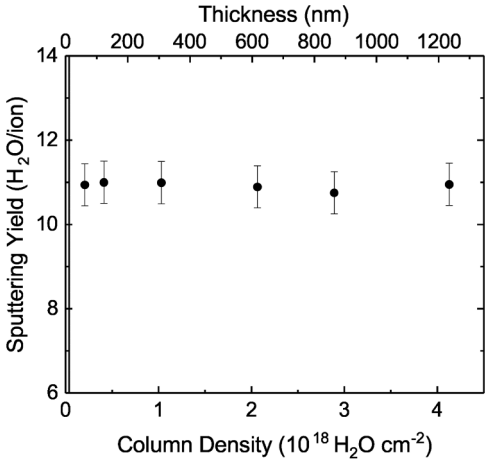

Fig. 3. Total sputtering yield for a H_2O-ice irradiated with 3 keV Ar^+ at 80 K as a function of column density. Film thickness was calculated assuming a film density of 1 g cm^{-3}. The solid black vertical line on the left of the figure indicates the range of a 3 keV Ar^+.

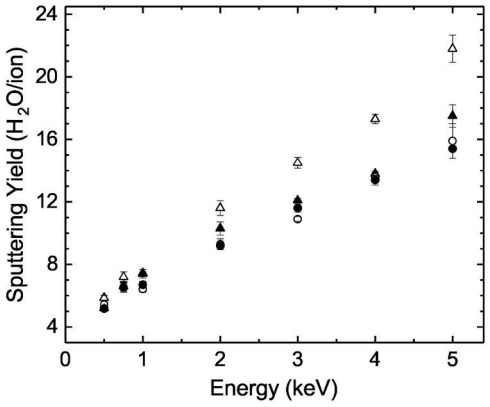

Fig. 4. Total sputtering yield for 2.9×10^{18} H_2O cm^{-2} samples as a function of incident ion energy for 120 K(△), 100 K(▲), 80 K(◦), and 40 K(●).

to those within the literature. Fig. 5 shows our total sputtering yields as a function of energy at an irradiation temperature of 80 K, along with others compiled in [10]. All yields were acquired at irradiation temperatures between 60 and 80 K and corrected for angular dependence by multiplying by a factor of $\cos(\theta)^{1.78}$, where θ is the angle of incidence for the ions [10]. Our experimental yields are consistent with previous studies and for the most part are transected by the theoretical values predicted by [10] (i.e. Eq. (3), Fig. 5 solid black line).

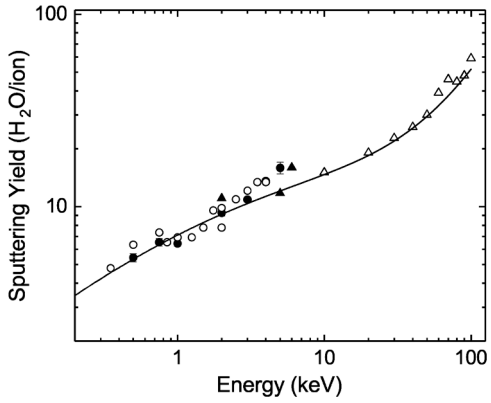

Fig. 5. Comparison of our experimental total sputtering yields with those found in literature and compiled in [10]. The symbols correspond to: this study Ar^+ 80 K (●), [7] Ar^+ 78 K (▲), [9] Ar^+ 60 K (△), and [10] Ar^+ 80 K (◦).

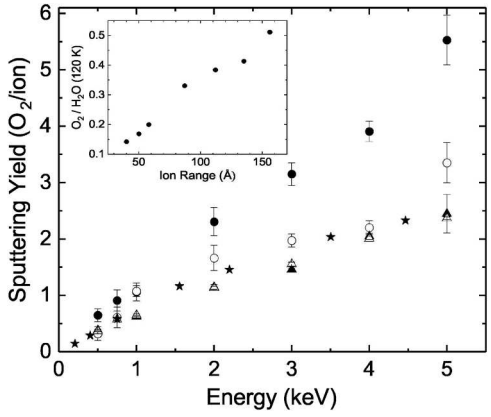

Fig. 6. Calculated O_2 sputtering yields for 2.9×10^{18} H_2O cm^{-2} samples as a function of incident projectile energy for 40 (△), 80 (▲), 100 (◦) and 120 K (●). Additionally, data from Teolis et al. [20] is shown for T ≤ 20 K (★). Inset: Derived O_2/H_2O ratio at 120 K as a function of ion range.

3.3. Energy and temperature dependence of the sputtered O_2 component

While the model comparison shown in Fig. 5 assumes the total yield is in the form of H_2O, we can also estimate the portion of the yield that is due to sputtered O_2 using the approach described in Section 2.3. In Fig. 6, we show the O_2 sputtering yield as a function of energy for 40, 80, 100 and 120 K. The observation that the O_2 yield increases as a function of energy is expected from the modeling predictions. We remind the reader that the values at 40 and 80 K are derived from our total mass loss (Fig. 4) and the O_2/H_2O ratios given in Table 1. Interestingly, even at 100 K the O_2 is still primarily driven by this intrinsic O_2, as the enhanced O_2 is on average 20 % of the total O_2 yield. As expected, the contribution from enhanced O_2 at 120 K is more important, as on average it is about half of the total O_2 yield. Additionally, we also find that the $Y_{O_2}(120\,K)/Y_{O_2}(40\,K)$ at each energy studied is within about 20% of the average value, supporting previous conclusions that the temperature dependence in the O_2 yield is independent of the particle energy [27].

An additional way to look at the data in Fig. 6 is to evaluate how the O_2/H_2O ratio in the sputtered flux changes with ion range. While this is somewhat uninformative at low temperatures, as those ratios were taken directly from the model (Table 1), we plot this for 120 K in the inset of Fig. 6. The ratio increases nearly linearly from ~ 0.15 at 0.5 keV to ~ 0.5 at 5 keV. This increase of the ratio with increasing ion range (and hence energy) is a consequence of the O_2 concentration profile, as previous depth profiling studies have convincingly shown that radiolytic O_2 is most efficiently produced within the first few hundred angstroms below

the surface ice and the concentration falls exponentially as one moves into the bulk [11,28]. Generally, this profile appears to be related to the production and out diffusion of H_2 as hydrogen loss makes the altered region more oxidizing, leading to the more efficient formation of O_2 [11, 28,37]. Furthermore, the observation that our measured ratios with 3–5 keV Ar^+ are similar to what has been seen previously using more highly penetrating Ar^+ at similar temperatures [11,38], suggests that our observed trend with energy would quickly level out or possibly drop slightly above 5 keV. This prediction seems reasonable considering that 5 keV Ar^+ has a range of ~150 Å in H_2O-ice (Table 2) and thus is likely probing to a depth where the radiolytic O_2 is most efficiently produced.

Finally, we can also compare these derived O_2 yields to the only previous laboratory study that estimates the O_2 yield for Ar^+ in our energy range [20]. Although these experiments were only performed at $T \leq 20$ K, these values should be comparable to our low irradiation temperatures (≤ 80 K), where the yield has been estimated to be nearly independent of temperature [34]. These values are overlayed with our data in Fig. 6 after accounting for the dependence of the sputtering yield on ion incidence angle [10]. The overall agreement with our data is excellent, as the values are no worse than within 10-15% of one another.

3.4. Comparison to theoretical predictions of the sputtered O_2 component

Besides comparing our work to previous laboratory results, we were interested in determining whether the most recent theoretical model predicting O_2 sputtering yields from H_2O-ice would agree with our newly derived data. In Fig. 7, we compare the model predictions with our O_2 sputtering yields at 40 and 120 K, as well as those given for ≤ 20 K [20]. The two tunable parameter values used were $g^0_{O_2} = 0.005$ O_2 eV^{-1} and $x_0 = 29$ Å, where the estimates of x_0 (as well as r_0) assume the H_2O-ice density is 1 g cm^{-3} [27]. While the previous laboratory results are well fit by the model, our data does not yield satisfactory results.

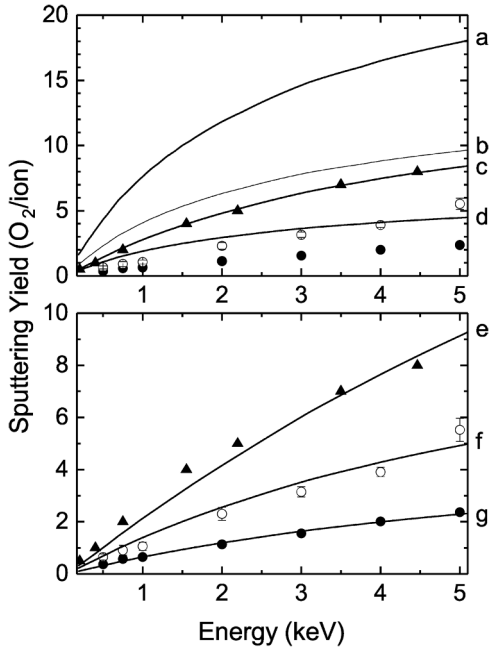

Fig. 7. Comparison of our derived O_2 total sputtering yields at 40 K (•) and 120 K (◦), as well as those given in Teolis et al. 2010 (▲) with the yields predicted from Eq. (4). Top: solid lines (a-d) correspond to using Eq. (4) along with the best fit parameters (g_0, x_0, Q, T, β): a) 0.005 O_2 eV^{-1} 29 Å, 0.06 eV, 120 K, 0°; b) 0.005 O_2 eV^{-1} 29 Å, 0.07 eV, 120 K, 0°; c) 0.005 O_2 eV^{-1} 29 Å, 0.07 eV, 12 K, 60°; d) 0.005 O_2 eV^{-1} 29 Å, 0.07 eV, 40 K, 0°. Bottom: solid lines (e-g) correspond to fits after modifying Eq. (4) (see text) along with the best fit parameters: (g_0, x_0, Q, T, β): e) 0.001 O_2 eV^{-1} 90 Å, 0.07 eV, 12 K, 60°; f) 0.001 O_2 eV^{-1} 90 Å, 0.07 eV, 120 K, 0°; g) 0.001 O_2 eV^{-1} 90 Å, 0.07 eV, 40 K, 0°.

Specifically, our measurements at 40 K are systematically lower than the predicted values by a factor of three, while our 120 K experiments are lower by about a factor of five to eight. The latter can be improved substantially if we adjust the effective activation energy (Q) in the temperature term from 0.06 eV to 0.07 eV, which is within the uncertainty given previously [27], although the fit still is poor (see Fig. 7 top). Superficially, the difference between our laboratory results and the model is somewhat surprising, as our Ar^+ O_2 experimental yields compare well with those derived in [20] after correcting for the incidence angle (see above). However, this appears to be due to the difference in projectile range in the two experiments, as even at our lower irradiation energies ions penetrate to depths that fall into the "high--range" limit producing errors by as much as 50% [27] or in our case slightly higher.

As the propensity of the model to overestimate the O_2 sputtering yield when the $r_0\cos\beta >> x_0$ is likely related to the approximation that the energy is deposited uniformly over the ion range [27], we investigated whether a simple modification to Eq. (4) and its best fit parameters could improve the fits shown in Fig. 7 (top). Efforts to do this by only modifying $g^0_{O_2}$ and x_0 were, as expected, unsuccessful. Additionally, adjusting these two parameters along with replacing the term representative of the average deposited energy ($\epsilon/r_0\cos\beta$) with a simple piecewise function that introduces an additional term of $x_0/(r_0(\cos\beta))$ when $x_0 \geq 1$, in an attempt to account for the predicted relation between the predicted sputtering yield of O_2 at high ion ranges, were only marginally better considering the quality of the fits for both datasets. Interestingly, we found that optimizing the model with $g^0_{O_2} = 0.001$ O_2 eV^{-1} and $x_0 = 90$ Å after changing the average deposited energy term from $\epsilon/(r_0\cos\beta)$ to $\epsilon/(r_0(\cos\beta)^{2.5})$ for all ion ranges improved the fit for our low temperature and high temperature data sets substantially, while only marginally changing the low temperature results where irradiation was performed at a high angle of incidence (Fig. 7 bottom). More quantitatively, we found the difference between the model prediction and three laboratory datasets to be typically within ~ 10% and no worse than within 30%. While the significant downward adjustment in $g^0_{O_2}$ cannot be reconciled with laboratory estimates [27], the larger value for x_0, which is an approximation of the depth over which O_2 is produced, is reasonable considering our results on the variation of the O_2/H_2O sputtered ratio as a function of ion energy as well as those from previous depth profiling studies [11,28]. Although this empirical fit may prove to be fortuitous, it suggests that careful consideration of how the energy is deposited over the region where O_2 is formed could substantially extend the accuracy of the existing model at large ion ranges. Until then, it is of interest to determine whether this empirical adjustment would generally work when other parameters are varied (incidence angles, ions, energies, etc.), something that could be tested with additional laboratory studies.

3.5. Astrophysical implications

Icy moons in the outer Solar System are bombarded with charged particles of varying energies that can erode and alter the composition of the surface ice. For Europa, an icy moon of Jupiter, Cassidy et al. [21] used results from previous laboratory studies to estimate the sputtering rate of the surface H_2O, as well as the sputtering rate of radiolytically-produced H_2 and O_2. They found that while the majority of the sputtered H_2O is caused by fast S^{n+} ions, the sputtered O_2 and H_2 are primarily caused by slower O^{n+} and S^{n+} ions, which not only deposit substantial energy near the surface where these products are primarily formed, but also bombard the surface at a significantly higher rate than do the fast ions [21]. Our new data here, which suggests that the sputtered O_2 produced by low-energy ions at the higher temperatures relevant to Europa [39] is about a factor of five lower than current theoretical predictions (assuming the use of Q = 0.06 eV), suggests that contributions from these low-energy ions may have been significantly

overestimated. For the time being, our new empirical fit may allow for more accurate predictions of sputtering yields. However, we point out that accurate modeling of the sputtering of extraterrestrial icy surfaces needs to take into account other factors (e.g., presence of a regolith, possibility of redeposition, and temperature variations), besides the sputtering yield. Thus, a more quantitative assessment on the degree to which our new laboratory data, as well as our new empirical estimate would alter previous estimates of O_2 erosion rates will require future modeling efforts.

4. Conclusions

We report sputtering yields for 0.5–5 keV Ar^+ at irradiation temperatures between 40 and 120 K. Below 80 K, our total sputtering yields cluster around the theoretical sputtering yields predicted by the Famá et al. 2008 model and are generally consistent with previous laboratory studies. In addition, we also estimate the sputtering yield of radiolytically produced O_2 as a function of energy for temperatures between 40 and 120 K. At 120 K, we find that the O_2/H_2O sputtered ratio increases nearly linearly with the ion range from about 0.15 to 0.5, which we attribute to the ions stopping at depths where O_2 is still efficiently being produced below the surface, consistent with previous depth profiling studies. Although our O_2 sputtering results agree well with the only comparable laboratory study, we find that theoretical models over predict the values by a factor of three or more, which is likely a consequence of the assumption that our more highly penetrating ions deposit energy uniformly throughout the sample. However, we find that making a small adjustment to this model allows us to fit the experimental data to within $\sim$ 10% in most cases and no worse than 30% in any case. Although the adjustment is primarily empirical, it could be useful to refine models predicting the sputtering of O_2 in icy extraterrestrial environments. This may be particularly important for Europa, where low-energy ions are predicted to be the primary ion producing O_2 from sputtering of the surface H_2O-ice.

CRediT authorship contribution statement

Patrick D. Tribbett: Conceptualization, Methodology, Software, Investigation, Formal analysis, Writing - original draft. **Mark J. Loeffler:** Conceptualization, Methodology, Software, Formal analysis, Writing - review & editing, Funding acquisition.

Declaration of Competing Interest

The authors declare that they have no known competing financial interests or personal relationships that could have appeared to influence the work reported in this paper.

Acknowledgements

This research was supported by NSF Grant # 1821919. Data can be found in Northern Arizona University's long-term repository (https://openknowledge.nau.edu/5536/).

Supplementary material

Supplementary material associated with this article can be found, in the online version, at doi:10.1016/j.susc.2021.121797.

References

[1] P. Sigmund, Theory of sputtering. I. Sputtering yield of amorphous and polycrystalline targets, Phys. Rev. 184 (2) (1969) 383.
[2] W. Brown, L. Lanzerotti, J. Poate, W. Augustyniak, "Sputtering" of ice by MeV light ions, Phys. Rev. Lett. 40 (15) (1978) 1027.
[3] R. Haring, A. Kolfschoten, A. De Vries, Chemical sputtering by keV ions, Nucl. Instrum. Meth. B 2 (1-3) (1984) 544–549.
[4] C. Plainaki, A. Milillo, A. Mura, S. Orsini, S. Massetti, T. Cassidy, The role of sputtering and radiolysis in the generation of Europa exosphere, Icarus 218 (2) (2012) 956–966.
[5] R. Johnson, M. Burger, T. Cassidy, F. Leblanc, M. Marconi, W. Smyth, Composition and detection of Europa's sputter-induced atmosphere. Europa, University of Arizona Press, Tucson, 2009, pp. 507–527.
[6] R. Johnson, J. Luhmann, R. Tokar, M. Bouhram, J. Berthelier, E. Sittler, J. Cooper, T. Hill, H. Smith, M. Michael, et al., Production, ionization and redistribution of O2 in Saturn's ring atmosphere, Icarus 180 (2) (2006) 393–402.
[7] J. Christiansen, D.D. Carpini, I. Tsong, Sputtering of ices by keV ions, Nucl. Instrum. Meth. B 15 (1-6) (1986) 218–221.
[8] M. Shi, R. Baragiola, D. Grosjean, R. Johnson, S. Jurac, J. Schou, Sputtering of water ice surfaces and the production of extended neutral atmospheres, J. Geophys. Res. Planets 100 (E12) (1995) 26387–26395.
[9] R.A. Baragiola, R.A. Vidal, W. Svendsen, J. Schou, M. Shi, D. Bahr, C. Atteberrry, Sputtering of water ice, Nucl. Instrum. Meth. B 209 (2003) 294–303.
[10] M. Famá, J. Shi, R. Baragiola, Sputtering of ice by low-energy ions, Surf. Sci. 602 (1) (2008) 156–161.
[11] B. Teolis, R.A. Vidal, J. Shi, R.A. Baragiola, Mechanisms of O_2 sputtering from water ice by keV ions, Phys. Rev. B 72 (24) (2005) 245422.
[12] D. Bahr, M. Famá, R.A. Vidal, R.A. Baragiola, Radiolysis of water ice in the outer solar system: sputtering and trapping of radiation products, J. Geophys. Res. Planets 106 (E12) (2001) 33285–33290.
[13] R.A. Vidal, B. Teolis, R.A. Baragiola, Angular dependence of the sputtering yield of water ice by 100 keV proton bombardment, Surf. Sci. 588 (1-3) (2005) 1–5.
[14] A. Bar-Nun, G. Herman, M. Rappaport, Y. Mekler, Ejection of H_2O, O_2, H_2 and H from water ice by 0.5–6 keV H^+ and Ne^+ ion bombardment, Surf. Sci. 150 (1) (1985) 143–156.
[15] E.A. Muntean, P. Lacerda, T.A. Field, A. Fitzsimmons, W.C. Fraser, A.C. Hunniford, R.W. McCullough, A laboratory study of water ice erosion by low-energy ions, Mon. Not. R. Astron. Soc. 462 (3) (2016) 3361–3367.
[16] R.M. Meier, M.J. Loeffler, Sputtering of water ice by keV electrons at 60 K, Surf. Sci. 691 (2020) 121509.
[17] A. Galli, A. Vorburger, P. Wurz, A. Pommerol, R. Cerubini, B. Jost, O. Poch, M. Tulej, N. Thomas, 0.2 to 10 keV electrons interacting with water ice: radiolysis, sputtering, and sublimation, Planet. Space Sci. 155 (2018) 91–98.
[18] H.-G. Heide, On the irradiation of organic samples in the vicinity of ice, Ultramicroscopy 7 (3) (1982) 299–300.
[19] H.-G. Heide, Observations on ice layers, Ultramicroscopy 14 (3) (1984) 271–278.
[20] B. Teolis, G.H. Jones, P. Miles, R. Tokar, B. Magee, J. Waite, E. Roussos, D. Young, F. Crary, A.J. Coates, et al., Cassini finds an oxygen–carbon dioxide atmosphere at Saturn's icy moon Rhea, Science 330 (6012) (2010) 1813–1815.
[21] T. Cassidy, C. Paranicas, J. Shirley, J. Dalton III, B. Teolis, R. Johnson, L. Kamp, A. Hendrix, Magnetospheric ion sputtering and water ice grain size at Europa, Planet. Space Sci. 77 (2013) 64–73.
[22] R.A. Baragiola, Sputtering: survey of observations and derived principles, Philos. T. R. Soc. A 362 (1814) (2004) 29–53.
[23] W. Brown, W. Augustyniak, E. Brody, B. Cooper, L. Lanzerotti, A. Ramirez, R. Evatt, R. Johnson, Energy dependence of the erosion of H_2O ice films by H and He ions, Nucl. Instrum. Meth. 170 (1-3) (1980) 321–325.
[24] J. Boring, R. Johnson, C. Reimann, J. Garret, W. Brown, K. Marcantonio, Ion-induced chemistry in condensed gas solids, Nucl. Instrum. Methods Phys. Res. 218 (1-3) (1983) 707–711.
[25] C. Reimann, J. Boring, R. Johnson, J. Garrett, K. Farmer, W. Brown, K. Marcantonio, W. Augustyniak, Ion-induced molecular ejection from D_2O ice, Surf. Sci. 147 (1) (1984) 227–240.
[26] F. Rocard, J. Bénit, J. Bibrtng, D. Ledu, R. Meunier, Erosion of ices: physical and astrophysical discussion, Radiat. Effects 99 (1-4) (1986) 97–104.
[27] B. Teolis, C. Plainaki, T. Cassidy, U. Raut, Water ice, O_2, H_2 and H_2O_2 radiolysis and sputtering yields for any projectile species, energy or temperature: a model for icy astrophysical bodies, J. Geophys. Res., Planets 122 (10) (2017) 1996–2012.
[28] B. Teolis, J. Shi, R. Baragiola, Formation, trapping, and ejection of radiolytic O_2 from ion-irradiated water ice studied by sputter depth profiling, J. Chem. Phys. 130 (13) (2009) 134704.
[29] M.J. Loeffler, P.D. Tribbett, J.F. Cooper, S.J. Sturner, A possible explanation for the presence of crystalline H_2O-ice on Kuiper belt objects, Icarus 351 (2020) 113943.
[30] M. Sceats, S. Rice, In Water, A Comprehensive Treatise, in: F. Franks (Ed.) 7, Plenum Press, New York, 1982, p. 83, vol.
[31] D. Brown, S.M. George, C. Huang, E. Wong, K.B. Rider, R.S. Smith, B.D. Kay, H_2O condensation coefficient and refractive index for vapor-deposited ice from molecular beam and optical interference measurements, J. Phys. Chem. 100 (12) (1996) 4988–4995.
[32] C.-S. Lu, O. Lewis, Investigation of film-thickness determination by oscillating quartz resonators with large mass load, J. Appl. Phys. 43 (11) (1972) 4385–4390.
[33] W. Brown, W. Augustyniak, E. Simmons, K. Marcantonio, L. Lanzerotti, R. Johnson, J. Boring, C. Reimann, G. Foti, V. Pirronello, Erosion and molecule formation in condensed gas films by electronic energy loss of fast ions, Nucl. Instrum. Meth. Phys. Res. 198 (1) (1982) 1–8.
[34] W. Brown, W. Augustyniak, K. Marcantonio, E. Simmons, J. Boring, R. Johnson, C. Reimann, Electronic sputtering of low temperature molecular solids, Nucl. Instrum. Meth. B 1 (2-3) (1984) 307–314.
[35] J.F. Ziegler, M.D. Ziegler, J.P. Biersack, SRIM–the stopping and range of ions in matter (2010), Nucl. Instrum. Methods Phys. Res.Sect. B 268 (11–12) (2010) 1818–1823.
[36] J. Shi, M. Famá, B. Teolis, R. Baragiola, Ion-induced electrostatic charging of ice, Nucl. Instrum. Meth. B 268 (19) (2010) 2888–2891.

[37] R. Johnson, T. Quickenden, P. Cooper, A. McKinley, C. Freeman, The production of oxidants in Europa's surface, Astrobiology 3 (4) (2003) 823–850.
[38] R. Baragiola, C. Atteberry, C. Dukes, M. Famá, B. Teolis, Atomic collisions in solids: astronomical applications, Nucl. Instrum. Meth. B 193 (1-4) (2002) 720–726.
[39] J.R. Spencer, L.K. Tamppari, T.Z. Martin, L.D. Travis, Temperatures on Europa from galileo photopolarimeter-radiometer: nighttime thermal anomalies, Science 284 (5419) (1999) 1514–1516.